Estimating Channels By Transmitting Pilots From Reconfigurable Intelligent Surface

Yanze Zhu[1], Yang Liu[1*], Qingqing Wu[2], and Qingjiang Shi[3]
1: School of Information and Communication Engineering, Dalian University of Technology
2: Department of Electronic Engineering, Shanghai Jiao Tong University
3: School of Software Engineering, Tongji University, and Shenzhen Research Institute of Big Data, Shenzhen, China
Emails: {5476z4969y5283z@mail.dlut.edu.cn, yangliu_613@dlut.edu.cn, qingqingwu@sjtu.edu.cn, qing.j.shi@gmail.com}

***Abstract*—The rising reconfigurable intelligent surface (RIS) is a promising technology and a multitude of literature focuses on its channel estimation (CE), which is a critical and challenging task. Most existing works adopt a type of "cascaded channel" training scheme, where the "two-hop" channel cascaded by RIS is treated as one and measured by one shot. As unveiled by the latest researches, however, the concatenated channel suffers from severe fading loss and hence seriously degrades the CE precision. To resolve this difficulty, this paper proposes a novel training scheme. Specifically, being equipped with one transmit RF chain, the RIS broadcasts pilot signals to all other devices during the training period. This novel scheme can overcome double fading loss at a low hardware cost. The pilot design of the newly proposed training scheme is a difficult quartic optimization problem and we develop a gradient descent (GD) based solution to resolve it. Numerical results verify the effectiveness of our solution and demonstrate our training scheme can significantly outperform the traditional cascaded channel training method.**

***Index Terms*—Reconfigurable intelligent surface (RIS), channel estimation (CE), gradient descent (GD), pilot design.**

I. Introduction

A. Background

The emerging reconfigurable intelligent surface (RIS) [1], also well-known as intelligent reflecting surface (IRS) [2], has been widely studied in both academia and industry recently, which has been envisioned as a promising technology for the next generation of wireless communication systems. With its elements' phase-shifts being wisely configured, the RIS can provide *passive* beamforming gain at a low expense of hardware and energy [3].

Although the RIS can greatly benefit the communication network, its phase-shift configuration needs be carefully designed, which requires channel status information (CSI). The channel estimation (CE) of the RIS is especially difficult due to its lackness of signal transmitting/processing capability. Therefore, a rich body of literature concentrates on designing CE schemes tailored to RIS, e.g., [4]-[9]. Among all the existing works, one dominant class of methods belongs to the so-called "cascaded channel" scheme. As proposed in these schemes, the multiplicative effect channel obtained by concatenating the "two-hop" channels through RIS is acquired as a whole [4]-[6]. For instance, the authors of [4] decompose the RIS cascaded channel into rank-one subchannels and design pilot signals via adjusting RIS phase-shifting to optimize the mean square error (MSE) performance of least square (LS) estimator. The work [5] investigates pilot sequence designs to minimize MSE of the cascaded channel based on both linear minimum mean square error (LMMSE) estimator and deep neutral network estimator, and shows that discrete Fourier transform (DFT) pilots can achieve nearly optimal MSE. The authors of [6] study CE in a multi-user system aided by RIS. Via taking advantage of the fact that the link between the base station (BS) and RIS is common among all users' cascaded channels, [6] develops a three-stage CE scheme with low training overhead.

Besides the aforementioned cascaded training mainstream, there still exist a number of *active* CE schemes, i.e., via introducing active components (e.g. receiving RF-chain, signal processing unit, etc.) to acquire CSI [7]-[9]. For example, the paper [7] embeds sensors into the element array of the RIS to measure direct channels. The authors of [8] introduce one single receiving RF-chain into RIS and develop a compressive sensing (CS) based CE algorithm. The work [9] installs active sensors arranged in "L" shape in the uniform planar element array of RIS to sense the direct RIS channels.

B. Motivation

Along with research deepening, some important characteristics of RIS have been unveiled recently. Especially, one predominant feature of RIS is the severe fading loss [10]. As analyzed in [10], the cascaded RIS channel experiences severe attenuation due to the multiplicative nature of the two-hop links, which is named as *double-fading* effect in [10]. As indicated by the Cramer-Rao lower bound analysis [1], the CE MSE is inversely proportional to signal-to-noise-ratio (SNR). Therefore, the double-fading effect of RIS indeed severely degrades the CE performance of the cascaded channel training scheme. To combat the double fading curse, the work [11] proposes to use amplifiers at the RIS to emit, instead of reflecting, signals. Similarly, recall the works [7]-[9] introduce active components to RIS to realize sensing direct channels. Inspired by these works, we propose to equip the RIS with

* Corresponding author.

The work of Yang Liu was supported in part by Grant DUT20RC(3)029 and in part by the Open Research Project Programme of the State Key Laboratory of Internet of Things for Smart City (University of Macau) under Grant SKLIoTSC(UM)-2021-2023/ORP/GA01/2022.

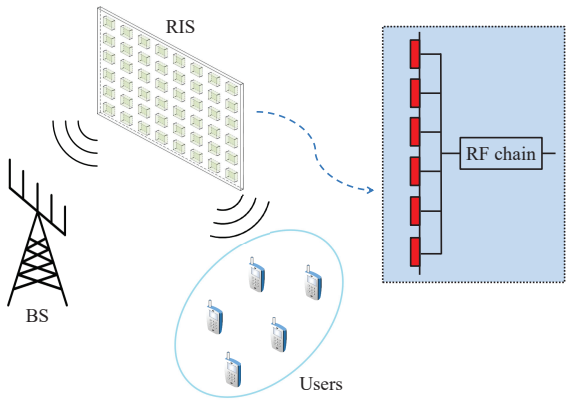

Fig. 1. RIS having TX RF-chain emits pilot signals.

one single transmit (TX) RF-chain, which entitles the RIS with signal transmission capability as shown in Fig. 1. During the training period, the RIS broadcasts pilot signals to the BS and all users. This novel training scheme has multiple advantages: i) effectively overcomes the double-fading loss; ii) maintains a low hardware cost of the RIS; iii) BS and users conduct CE simultaneously. To the best of our knowledge, this novel RIS CE scheme has never been considered in the literature.

II. System Model and Problem Formulation

A. System Setting

As illustrated in Fig. 1, consider a time division duplex (TDD) cellular system which consists of a BS equipped with $M_{\rm B}$ antennas, K single-antenna users and a RIS containing $M_{\rm R}$ reflecting elements. The sets of users and RIS elements are defined as $\mathcal{K} \triangleq \{1,\cdots,K\}$ and $\mathcal{M} \triangleq \{1,\cdots,M_{\rm R}\}$, respectively. Moreover, we denote $\mathbf{G} \in \mathbb{C}^{M_{\rm B}\times M_{\rm R}}$ and $\mathbf{h}_k \in \mathbb{C}^{M_{\rm R}},\ k \in \mathcal{K}$, as the channels between the BS and the RIS and between the RIS and the kth user, respectively. Note that our setting does not consider the direct channels connecting the BS and mobile users. In fact, these direct links' CSI can be easily acquired by following the standard CE procedure for conventional cellular systems without RIS [1].

As previously discussed, one TX RF-chain is built in the RIS device to entitle it with transmission capability, as shown in Fig. 1. During the channel training period, every RIS element is switched to connecting the single RF chain and adjusts the signal's phase before emitting over the air. Specifically, denote the RF-chain signal as a complex scalar $\sqrt{\alpha}e^{j\theta_0}$ with $\sqrt{\alpha}$ and θ_0 representing the amplitude and phase, respectively. Therefore, the emitted signal from the RIS can be expressed as $\boldsymbol{\psi} \triangleq [\sqrt{\alpha}e^{j(\theta_0+\theta_1)},\cdots,\sqrt{\alpha}e^{j(\theta_0+\theta_{M_{\rm R}})}]^{\rm T}$ with $\theta_i,\ i \in \mathcal{M}$, being the phase shift yielded by the ith element. Since the pilot signal is predefined, we can just assume $\theta_0 = 0$ without loss of generality.

B. Training Procedure

Based on the above, we elaborate the proposed RIS-transmit-based CSI acquisition procedure. The training period is composed of T consecutive time slots. Within each time slot, the RIS emits one pilot symbol, which is phase-modulated by the RIS elements, to the BS and all users. Specifically, denoting $\mathcal{T} \triangleq \{1,\cdots,T\}$, we can express the transmitted signal in the tth time slot as

$$\mathbf{x}^{(t)} = \sqrt{\alpha_t}\boldsymbol{\phi}^{(t)},\ t \in \mathcal{T}, \tag{1}$$

where $\boldsymbol{\phi}^{(t)} \triangleq [e^{j\theta_1^{(t)}},\cdots,e^{j\theta_{M_{\rm R}}^{(t)}}]^{\rm T}$.

After collecting all T pilot symbols from the RIS simultaneously, the BS and all users conduct signal processing and obtain the estimate of their own channel connecting the RIS. This procedure will be detailed in the sequel.

In the tth time interval, the BS receives the signal from the RIS which reads as

$$\mathbf{y}_{\rm B}^{(t)} = \mathbf{G}\boldsymbol{\psi}^{(t)} + \mathbf{n}_{\rm B}^{(t)},\ t \in \mathcal{T}, \tag{2}$$

where $\mathbf{n}_{\rm B}^{(t)},\ t \in \mathcal{T}$, represents the thermal noise at the BS and $\mathbf{n}_{\rm B}^{(t)} \sim \mathcal{CN}(\mathbf{0},\boldsymbol{\Sigma}_{\rm B})$ with the positive definite matrix $\boldsymbol{\Sigma}_{\rm B}$ denoting the covariance matrix of the noise which is assumed to be known. Besides, we assume that $\mathbf{n}_{\rm B}^{(t)}$'s with different t are independent for simplicity. To fully determine the channel $\mathbf{G}$, the length of the pilot sequence T should satisfy $T \geq M_{\rm R}$. For reducing training's overhead, we just assume that $T = M_{\rm R}$. By collecting all T observations and stacking them in a column-by-column manner, the training data obtained by the BS can be represented as

$$\mathbf{Y}_{\rm B} = \mathbf{G}\boldsymbol{\Psi} + \mathbf{N}_{\rm B}, \tag{3}$$

where $\mathbf{Y}_{\rm B} \triangleq [\mathbf{y}_{\rm B}^{(1)},\cdots,\mathbf{y}_{\rm B}^{(T)}]$, $\boldsymbol{\Psi} \triangleq [\boldsymbol{\psi}^{(1)},\cdots,\boldsymbol{\psi}^{(T)}]$, $\mathbf{N}_{\rm B} \triangleq [\mathbf{n}_{\rm B}^{(1)},\cdots,\mathbf{n}_{\rm B}^{(T)}]$. Via vectorizing $\mathbf{Y}_{\rm B}$ and utilizing the formula $\mathsf{vec}(\mathbf{ABC}) = (\mathbf{C}^{\rm T}\otimes\mathbf{A})\mathsf{vec}(\mathbf{B})$, we obtain

$$\mathbf{y}_{\rm B} = \mathsf{vec}(\mathbf{Y}_{\rm B}) = (\boldsymbol{\Psi}^{\rm T}\otimes\mathbf{I}_{M_{\rm B}})\mathbf{g} + \mathbf{n}_{\rm B} = \mathsf{A}_{\rm G}(\boldsymbol{\Psi})\mathbf{g} + \mathbf{n}_{\rm B}, \tag{4}$$

where $\mathbf{g} \triangleq \mathsf{vec}(\mathbf{G})$, $\mathbf{n}_{\rm B} \triangleq \mathsf{vec}(\mathbf{N}_{\rm B})$, $\mathsf{A}_{\rm G}(\boldsymbol{\Psi}) \triangleq \boldsymbol{\Psi}^{\rm T}\otimes\mathbf{I}_{M_{\rm B}}$ and $\mathbf{I}_{M_{\rm B}}$ is defined as an $M_{\rm B}\times M_{\rm B}$ identity matrix.

Similarly, the compact form of the signals observed by the kth user during the whole period can be expressed as

$$\mathbf{y}_{{\rm U},k} = \boldsymbol{\Psi}^{\rm T}\mathbf{h}_k + \mathbf{n}_{{\rm U},k},\ k \in \mathcal{K}, \tag{5}$$

where $\mathbf{n}_{{\rm U},k} \triangleq [n_{{\rm U},k}^{(1)},\cdots,n_{{\rm U},k}^{(T)}]^{\rm T}$ and $n_{{\rm U},k}^{(t)},\ k \in \mathcal{K},\ t \in \mathcal{T}$, therein indicates the thermal noise at the kth user in the tth interval with $n_{{\rm U},k}^{(t)} \sim \mathcal{CN}(0,\sigma_{{\rm U},k}^2)$. For simplicity, it is assumed that each $n_{{\rm U},k}^{(t)}$ is independent to others for different users and time slots.

In this paper, we assume that the channels $\mathbf{g}$ and $\{\mathbf{h}_k\}_{k=1}^K$ have zero mean and known covariance matrices. Specifically, we denote $\mathbf{R}_{\rm G}$ and $\mathbf{R}_{{\rm h},k},\ k \in \mathcal{K}$, as covariance matrices of $\mathbf{g}$ and $\mathbf{h}_k,\ k \in \mathcal{K}$, respectively. Besides, it is reasonable to assume that the channels associated with the BS and users are mutually uncorrelated. With the linear receivers $\mathbf{W}_{\rm G}$ at the BS and $\mathbf{W}_{{\rm h},k},\ k \in \mathcal{K}$, at the kth user, the BS/every user obtains the linear estimate of their own channels given as follows

$$\hat{\mathbf{g}} = \mathbf{W}_{\rm G}^{\rm H}\mathbf{y}_{\rm B} = \mathbf{W}_{\rm G}^{\rm H}\mathsf{A}_{\rm G}(\boldsymbol{\Psi})\mathbf{g} + \mathbf{W}_{\rm G}^{\rm H}\mathbf{n}_{\rm B}, \tag{6}$$

$$\hat{\mathbf{h}}_k = \mathbf{W}_{\mathrm{h},k}^{\mathrm{H}}\mathbf{y}_{\mathrm{U},k} = \mathbf{W}_{\mathrm{h},k}^{\mathrm{H}}\mathbf{\Psi}^{\mathrm{T}}\mathbf{h}_k + \mathbf{W}_{\mathrm{h},k}^{\mathrm{H}}\mathbf{n}_{\mathrm{U},k},\ k\in\mathcal{K}, \quad (7)$$

whose covariance matrices are given as follows after some manipulations

$$\mathbf{C}_{\hat{\mathrm{G}}} = \mathbf{W}_{\mathrm{G}}^{\mathrm{H}}\mathsf{A}_{\mathrm{G}}(\mathbf{\Psi})\mathbf{R}_{\mathrm{G}}\mathsf{A}_{\mathrm{G}}^{\mathrm{H}}(\mathbf{\Psi})\mathbf{W}_{\mathrm{G}} + \mathbf{W}_{\mathrm{G}}^{\mathrm{H}}(\mathbf{\Sigma}_{\mathrm{B}}\otimes\mathbf{I}_{M_{\mathrm{R}}})\mathbf{W}_{\mathrm{G}}, \quad (8)$$

$$\mathbf{C}_{\hat{\mathrm{h}},k} = \mathbf{W}_{\mathrm{h},k}^{\mathrm{H}}\mathbf{\Psi}^{\mathrm{T}}\mathbf{R}_{\mathrm{h},k}\mathbf{\Psi}^{*}\mathbf{W}_{\mathrm{h},k} + \mathbf{W}_{\mathrm{h},k}^{\mathrm{H}}\mathbf{\Sigma}_{\mathrm{U},k}\mathbf{W}_{\mathrm{h},k}, k\in\mathcal{K}, \quad (9)$$

where $\mathbf{\Sigma}_{\mathrm{U},k} \triangleq \mathsf{Diag}(\sigma_{\mathrm{U},k}^2,\cdots,\sigma_{\mathrm{U},k}^2),\ k\in\mathcal{K}$.

C. Pilot Design Problem

After performing CE, mobile users feedback their local estimates to the BS. The effective cascaded channel by way of the RIS for each user is defined by $\mathbf{H}_{\mathrm{c},k} \triangleq \mathbf{G}\mathsf{Diag}(\mathbf{h}_k),\ k\in\mathcal{K}$, and its estimate is given as $\hat{\mathbf{H}}_{\mathrm{c},k} \triangleq \hat{\mathbf{G}}\mathsf{Diag}(\hat{\mathbf{h}}_k),\ k\in\mathcal{K}$. Based on $\{\hat{\mathbf{H}}_{\mathrm{c},k}\}_{k=1}^K$, the BS will determine the scheduling and beamforming for all users. Therefore, it is critical to minimize the estimation error between the estimate $\{\hat{\mathbf{H}}_{\mathrm{c},k}\}_{k=1}^K$ and its true value. To evaluate the estimation performance, the MSE matrix of $\hat{\mathbf{H}}_{\mathrm{c},k},\ k\in\mathcal{K}$, is defined as $\mathbf{C}_{\mathrm{H}_{\mathrm{c},k}} \triangleq \mathbb{E}\{\mathsf{vec}(\mathbf{H}_{\mathrm{c},k}-\hat{\mathbf{H}}_{\mathrm{c},k})\mathsf{vec}^{\mathrm{H}}(\mathbf{H}_{\mathrm{c},k}-\hat{\mathbf{H}}_{\mathrm{c},k})\},\ k\in\mathcal{K}$, and its value is determined as follows

$$\mathbf{C}_{\mathrm{H}_{\mathrm{c},k}} = \mathbf{R}_{\mathrm{G}}\odot(\mathbf{R}_{\mathrm{h},k}\otimes\mathbb{1}_{M_{\mathrm{B}}}) + \mathbf{C}_{\hat{\mathrm{G}}}\odot(\mathbf{C}_{\hat{\mathrm{h}}_k}\otimes\mathbb{1}_{M_{\mathrm{B}}})$$
$$-2\mathsf{Re}\{(\mathbf{R}_{\mathrm{G}}\mathsf{A}_{\mathrm{G}}^{\mathrm{H}}(\mathbf{\Psi})\mathbf{W}_{\mathrm{G}})\odot((\mathbf{R}_{\mathrm{h},k}\mathbf{\Psi}^{*}\mathbf{W}_{\mathrm{h},k})\otimes\mathbb{1}_{M_{\mathrm{B}}})\}, \quad (10)$$

where $\mathbb{1}_{M_{\mathrm{B}}}$ denotes an $M_{\mathrm{B}}\times M_{\mathrm{B}}$ matrix with all elements 1. Hence, the estimation MSE of the effective channel $\hat{\mathbf{H}}_{\mathrm{c},k},\ k\in\mathcal{K}$, is given as $\mathsf{Tr}\{\mathbf{C}_{\mathrm{H}_{\mathrm{c},k}}\},\ k\in\mathcal{K}$, which is actually a function of the pilot sequence $(\mathbf{\Phi},\mathbf{P})$, where $\mathbf{\Phi} \triangleq [\boldsymbol{\phi}^{(1)},\cdots,\boldsymbol{\phi}^{(T)}]^{\mathrm{T}}$, $\mathbf{P} \triangleq \mathsf{Diag}(\sqrt{\alpha_1},\cdots,\sqrt{\alpha_T})$ and we have $\mathbf{\Psi} = \mathbf{\Phi}\mathbf{P}$. Besides, we denote $\boldsymbol{\mathcal{W}}_{\mathrm{h}} \triangleq \{\mathbf{W}_{\mathrm{h},k}\}_{k=1}^K$.

Based on the aforementioned RIS-transmit based training scheme, we aim at minimizing the overall MSE of all users' effective channels $\{\hat{\mathbf{H}}_{\mathrm{c},k}\}_{k=1}^K$ via designing the pilot sequence and the linear receivers $(\mathbf{\Phi},\mathbf{P},\mathbf{W}_{\mathrm{G}},\boldsymbol{\mathcal{W}}_{\mathrm{h}})$. This problem can be formulated as the following optimization problem

$$(\mathcal{P}1): \min_{\mathbf{\Phi},\mathbf{P},\mathbf{W}_{\mathrm{G}},\boldsymbol{\mathcal{W}}_{\mathrm{h}}} \sum_{k=1}^K \frac{\mathsf{Tr}\{\mathbf{C}_{\mathrm{H}_{\mathrm{c},k}}(\mathbf{\Phi},\mathbf{P},\mathbf{W}_{\mathrm{G}},\boldsymbol{\mathcal{W}}_{\mathrm{h}})\}}{K} \quad (11)$$
$$\text{s.t. } \|\mathbf{\Phi}\mathbf{P}\|_{\mathrm{F}}^2 \le P_{\mathrm{RIS,max}}, \quad (11a)$$
$$|[\mathbf{\Phi}]_{i,j}| = 1,\ i,j\in\mathcal{M}, \quad (11b)$$
$$\alpha_t \ge 0,\ t\in\mathcal{T}, \quad (11c)$$

where $P_{\mathrm{RIS,max}}$ in (11a) represents the maximal transmit power of the TX RF-chain. The problem $(\mathcal{P}1)$ is highly challenging due to its nonconvex objective, which is indeed a quartic function in $(\mathbf{\Phi},\mathbf{P})$.

III. Proposed Algorithm

In the following, we resolve $(\mathcal{P}1)$ in a block coordinate descent (BCD) manner.

1) Optimize the phase shift matrix $\mathbf{\Phi}$

Fixing other variables, the optimization w.r.t. $\mathbf{\Phi}$ is given by

$$(\mathcal{P}2): \min_{\mathbf{\Phi}} \sum_{k=1}^K \mathsf{Tr}\{\mathbf{C}_{\mathrm{H}_{\mathrm{c},k}}(\mathbf{\Phi}|\mathbf{P},\mathbf{W}_{\mathrm{G}},\boldsymbol{\mathcal{W}}_{\mathrm{h}})\} \quad (12)$$
$$\text{s.t. } |[\mathbf{\Phi}]_{i,j}| = 1,\ i,j\in\mathcal{M}, \quad (12a)$$

which is non-convex due to the equality constraint (12a) and challenging to solve. Hence, we turn to investigate another optimization equivalent to $(\mathcal{P}2)$ which can be expressed as

$$(\mathcal{P}3): \min_{\mathbf{\Theta}} \sum_{k=1}^K \mathsf{Tr}\{\mathbf{C}_{\mathrm{H}_{\mathrm{c},k}}(\mathbf{\Theta}|\mathbf{P},\mathbf{W}_{\mathrm{G}},\boldsymbol{\mathcal{W}}_{\mathrm{h}})\} \quad (13)$$
$$\text{s.t. } [\mathbf{\Theta}]_{i,j}\in[0,2\pi],\ i,j\in\mathcal{M}, \quad (13a)$$

where $\mathbf{\Theta} \triangleq \angle(\mathbf{\Phi})$ and $\angle(\mathbf{\Phi})$ takes the value of phases of $\mathbf{\Phi}$'s entries in an element-wise manner. By noting that $e^{j(\theta+2n\pi)} = e^{j\theta},\ n\in\mathbb{Z}$, problem $(\mathcal{P}3)$ can be viewed as an unconstrained optimization problem w.r.t. $\mathbf{\Theta}$. Therefore, we adopt gradient descent (GD) algorithm to tackle $(\mathcal{P}3)$. Denote $\mathsf{g}(\mathbf{\Theta})$ as the objective of $(\mathcal{P}3)$. Then, the gradient descent of $\mathbf{\Theta}$ is conducted as

$$\mathbf{\Theta}^{(n+1)} := \mathbf{\Theta}^{(n)} - \eta_{\mathbf{\Theta}}^{(n)}\nabla_{\mathbf{\Theta}}\mathsf{g}(\mathbf{\Theta})|_{\mathbf{\Theta}=\mathbf{\Theta}^{(n)}}, \quad (14)$$

where $\eta_{\mathbf{\Theta}}^{(n)}$ is the step size for updating $\mathbf{\Theta}$. We leave the calculation of $\nabla_{\mathbf{\Theta}}\mathsf{g}(\mathbf{\Theta})$ in Appendix A. Lastly, $\mathbf{\Phi}^{(n+1)}$ is given by $\mathbf{\Phi}^{(n+1)} = e^{j\mathbf{\Theta}^{(n+1)}}$.

2) Optimize the power allocation $\mathbf{P}$

We proceed to study the optimization of power allocation $\mathbf{P}$ when other variables are given. Notice again $\mathbf{P} \triangleq \mathsf{Diag}(\sqrt{\alpha_1},\cdots,\sqrt{\alpha_T})$. Therefore, by defining $\mathbf{p} \triangleq \mathsf{diag}(\mathbf{P})$, the sub-problem to optimize power allocation can be expressed as

$$(\mathcal{P}4): \min_{\mathbf{p}\in\mathbb{R}^T} \sum_{k=1}^K \mathsf{Tr}\{\mathbf{C}_{\mathrm{H}_{\mathrm{c},k}}(\mathbf{p}|\mathbf{\Phi},\mathbf{W}_{\mathrm{G}},\boldsymbol{\mathcal{W}}_{\mathrm{h}})\} \quad (15)$$
$$\text{s.t. } \mathbf{p}^{\mathrm{T}}\mathbf{p} \le \frac{P_{\mathrm{RIS,max}}}{M_{\mathrm{R}}}, \quad (15a)$$
$$\mathbf{p} \ge \mathbf{0}. \quad (15b)$$

The objective of $(\mathcal{P}4)$ is non-convex and we still adopt GD-like method to attack it. Note that plain GD algorithm only applies to unconstrained optimization problem. For the constrained problem $(\mathcal{P}4)$, we adopt the gradient projection (GP) method. GP method is an iterative procedure. In each iteration, it performs two steps in order: i) gradient descent and ii) projection onto the feasible domain. Denoting the objective of $(\mathcal{P}4)$ as $\mathsf{h}(\mathbf{p})$, we elaborate these two steps in the following:

i) Gradient Descent: The variable $\mathbf{p}$ moves in the direction of negative derivative, i.e.

$$\mathbf{p}^{(n+1)} := \mathbf{p}^{(n)} - \eta_{\mathrm{p}}^{(n)}\nabla_{\mathbf{p}}\mathsf{h}(\mathbf{p})|_{\mathbf{p}=\mathbf{p}^{(n)}}, \quad (16)$$

where $\eta_{\mathrm{p}}^{(n)}$ is the step size for updating power allocation. The calculation of $\nabla_{\mathbf{p}}\mathsf{h}(\mathbf{p})$ is shown in Appendix B.

ii) Projection: After performing the update of $\mathbf{p}$ as shown above, there exists a risk that $\mathbf{p}^{(n+1)}$ moves out of the feasible domain identified by (15a) and (15b). Hence, we need project $\mathbf{p}^{(n+1)}$ onto the convex feasible domain of $(\mathcal{P}4)$, which means to solve the following optimization

$$(\mathcal{P}5): \min_{\mathbf{x}\in\mathbb{R}^T} \frac{1}{2}\|\mathbf{x}-\mathbf{p}^{(n+1)}\|_2^2 \quad (17)$$
$$\text{s.t. } \mathbf{x}^{\mathrm{T}}\mathbf{x} \le \frac{P_{\mathrm{RIS,max}}}{M_{\mathrm{R}}}, \quad (17a)$$

$$\mathbf{x} \geq \mathbf{0}. \tag{17b}$$

The optimal solution to $(\mathcal{P}5)$ is given by Lemma 1, whose proof is omitted due to limit of space.

Lemma 1. *If* $\|[\mathbf{p}^{(n+1)}]_+\|_2^2 \leq \frac{P_{\mathrm{RIS,max}}}{M_{\mathrm{R}}}$, *we have*

$$\mathbf{x}^\star = [\mathbf{p}^{(n+1)}]_+, \tag{18}$$

otherwise,

$$\mathbf{x}^\star = \sqrt{\frac{P_{\mathrm{RIS,max}}}{M_{\mathrm{R}}}} \frac{[\mathbf{p}^{(n+1)}]_+}{\|[\mathbf{p}^{(n+1)}]_+\|_2}, \tag{19}$$

where $[\mathbf{p}^{(n+1)}]_+ \triangleq \max\{\mathbf{p}^{(n+1)}, \mathbf{0}\}$ *in an element-wise manner.*

3) Optimize the linear receiver at the BS $\mathbf{W}_{\mathrm{G}}$

When other variables are given, the subproblem w.r.t. $\mathbf{W}_{\mathrm{G}}$ is indeed an unconstrained convex quadratic optimization problem. Therefore, by checking the first-order optimality condition of $\mathbf{W}_{\mathrm{G}}$, the newly obtained $\mathbf{W}_{\mathrm{G}}$ can be expressed in the closed-form as follows

$$\mathbf{W}_{\mathrm{G}} = \mathbf{J}_{\mathrm{G}} \mathbf{D}_{\mathrm{G},1} \mathbf{D}_{\mathrm{G},2}^{-1}, \tag{20}$$

where

$$\begin{aligned}
\mathbf{J}_{\mathrm{G}} &= (\mathsf{A}_{\mathrm{G}}(\mathbf{\Psi}) \mathbf{R}_{\mathrm{G}} \mathsf{A}_{\mathrm{G}}^{\mathrm{H}}(\mathbf{\Psi}) + \mathbf{\Sigma}_{\mathrm{B}} \otimes \mathbf{I}_{M_{\mathrm{R}}})^{-1} \mathsf{A}_{\mathrm{G}}(\mathbf{\Psi}) \mathbf{R}_{\mathrm{G}}, \\
\mathbf{D}_{\mathrm{G},1} &= \sum\nolimits_{k=1}^{K} \mathsf{Ddiag}((\mathbf{W}_{\mathrm{h},k}^{\mathrm{H}} \mathbf{\Psi}^{\mathrm{T}} \mathbf{R}_{\mathrm{h},k}) \otimes \mathbb{1}_{M_{\mathrm{B}}}), \\
\mathbf{D}_{\mathrm{G},2} &= \sum\nolimits_{k=1}^{K} \mathsf{Ddiag}(\mathbf{C}_{\hat{\mathrm{h}},k} \otimes \mathbb{1}_{M_{\mathrm{B}}}),
\end{aligned} \tag{21}$$

with $\mathsf{Ddiag}(\mathbf{X})$ constructing a diagonal matrix with its diagonal elements being those of the square matrix $\mathbf{X}$.

4) Optimize the linear receiver at every user $\mathcal{W}_{\mathrm{h}}$

Following the similar procedure of updating $\mathbf{W}_{\mathrm{G}}$, the solution to $\mathbf{W}_{\mathrm{h},k},\ k \in \mathcal{K}$, can also be obtained in a closed-form as follows (details are omitted for brevity)

$$\mathbf{W}_{\mathrm{h},k} = \mathbf{J}_{\mathrm{h},k} \mathbf{D}_{\mathrm{h},1} \mathbf{D}_{\mathrm{h},2}^{-1},\ k \in \mathcal{K}, \tag{22}$$

where

$$\mathbf{J}_{\mathrm{h},k} = (\mathbf{\Psi}^{\mathrm{T}} \mathbf{R}_{\mathrm{h},k} \mathbf{\Psi}^{*} + \mathbf{\Sigma}_{\mathrm{U},k})^{-1} \mathbf{\Psi}^{\mathrm{T}} \mathbf{R}_{\mathrm{h},k},\ k \in \mathcal{K}, \tag{23}$$

$\mathbf{D}_{\mathrm{h},1}$ and $\mathbf{D}_{\mathrm{h},2}$ are M_{R}-dimensional diagonal matrices with $[\mathbf{D}_{\mathrm{h},1}]_{m,m} = \sum_{n=1}^{M_{\mathrm{B}}} [\mathbf{W}_{\mathrm{G}}^{\mathrm{H}} \mathsf{A}_{\mathrm{G}}(\mathbf{\Psi}) \mathbf{R}_{\mathrm{G}}]_{(m-1)M_{\mathrm{B}}+n,(m-1)M_{\mathrm{B}}+n},\ m \in \mathcal{M}$, and $[\mathbf{D}_{\mathrm{h},2}]_{m,m} = \sum_{n=1}^{M_{\mathrm{B}}} [\mathbf{C}_{\hat{\mathrm{G}}}]_{(m-1)M_{\mathrm{B}}+n,(m-1)M_{\mathrm{B}}+n},\ m \in \mathcal{M}$, respectively.

The overall algorithm of solving $(\mathcal{P}1)$ based on GD is summarized in Algorithm 1.

Algorithm 1: Solving the problem $(\mathcal{P}1)$ based on GD

1: Initialize feasible $\mathbf{\Psi}^{(0)} = \mathbf{\Phi}^{(0)} \mathbf{P}^{(0)}$ and $t = 0$;
2: **repeat**
3: update $\mathbf{W}_{\mathrm{G}}^{(t+1)}$ by (20);
4: update $\mathcal{W}_{\mathrm{h}}^{(t+1)}$ by (22);
5: update $\mathbf{\Phi}^{(t+1)}$ by solving $(\mathcal{P}2)$ via GD procedure;
6: update $\mathbf{P}^{(t+1)}$ by solving $(\mathcal{P}4)$ via GP procedure;
7: set $\mathbf{\Psi}^{(t+1)} = \mathbf{\Phi}^{(t+1)} \mathbf{P}^{(t+1)}$;
8: $t := t + 1$;
9: **until** convergence

IV. Simulation Results

In this section, numerical results will be presented to verify the effectiveness of our algorithms and the benefit of the proposed RIS-TX training scheme. As illustrated in Fig. 2, we consider a system which includes a BS with $M_{\mathrm{B}} = 8$ antennas, $K = 4$ users and a RIS equipped with one TX RF-chain. Unless otherwise specified, $d_{\mathrm{B}} = \{d_{\mathrm{U},k}\}_{k=1}^{K} = d = 100\mathrm{m}$,

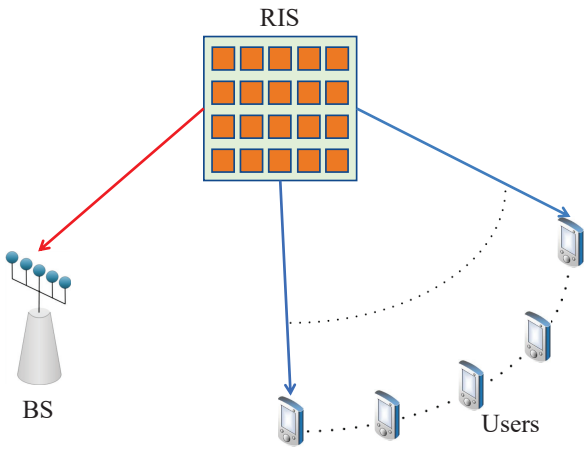

Fig. 2. Simulation scenario.

$\mathbf{\Sigma}_{\mathrm{B}} = \sigma_{\mathrm{B}}^2 \mathbf{I}_{M_{\mathrm{B}}}$, $\sigma_{\mathrm{B}}^2 = -90\mathrm{dBm}$, $\sigma_{\mathrm{U},k}^2 = -80\mathrm{dBm},\ k \in \mathcal{K}$, and we exploit the 3GPP Urban Micro standard to model the distance-dependent pathloss [12]

$$\mathsf{f}(d) = G_{\mathrm{t}} + G_{\mathrm{r}} - 37.5 - 22 \log_{10}(d/1\mathrm{m})\ [\mathrm{dB}], \tag{24}$$

where G_{t} and G_{r} indicate the antenna gains (in dBi) at the transmitter and the receiver, respectively.

Fig. 3 illustrates the convergence of Alg. 1. It can be observed that, the GD algorithm generally converges within several tens of iterations.

In Fig. 4, we investigate the impact of the transmit power $P_{\mathrm{RIS,max}}$ on the MSE performance. As suggested by the figure, the MSE decreases when the transmit power grows. Importantly, the results in Fig. 4 reflect that the pilot sequence yielded by our proposed algorithm outperforms the classical DFT codebook for RIS-TX training scheme. Note that the DFT sequence is nearly optimal for the classical cascaded CE scheme, as demonstrated by different literature [4]-[6].

Fig. 5 plots the impact of the number of reflecting elements on the CE performance. As shown in Fig. 5, given a specific $P_{\mathrm{RIS,max}}$, the CE performance degrades when the number of RIS elements M_{R} increases. This is because when M_{R} is large, the average power allocated to each element decreases, which deteriorates the estimation precision. Besides, as previously

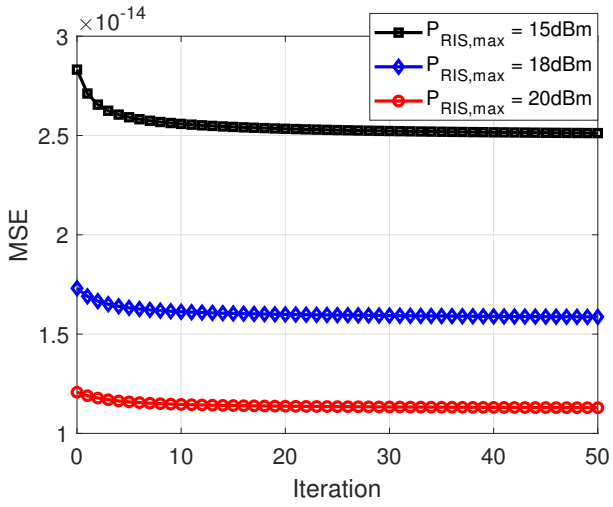

Fig. 3. Convergence of Alg. 1.

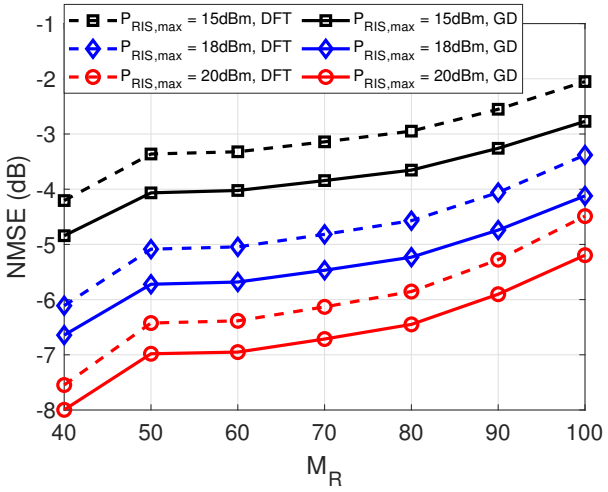

Fig. 5. The impact of M_{R} on the CE performance.

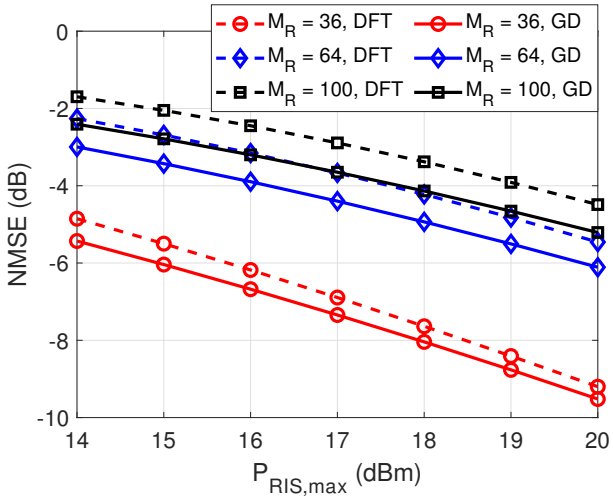

Fig. 4. The impact of $P_{\mathrm{RIS,max}}$ on the CE performance.

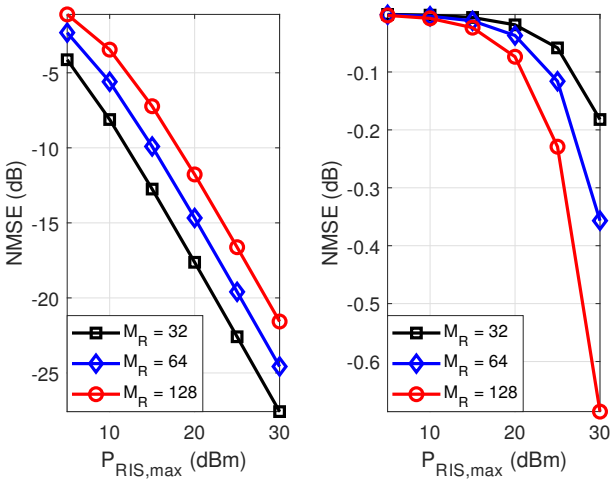

Fig. 6. RIS-TX training v.s. cascaded channel training: Impact of $P_{\mathrm{RIS,max}}$.

discussed, the pilot sequences yielded by our algorithm have superior performance than the DFT counterpart.

In Fig. 6, we compare the MSE performance of our proposed RIS-TX CE scheme and the standard cascaded channel training scheme [5], [6], where the left half presents CE performance associated with the RIS-TX training scheme while the right half plots that of the standard cascaded channel training. As suggested by Fig. 6, the proposed RIS-TX scheme significantly outperforms the cascaded channel training. This is because the double fading effect severely attenuates the pilot signals' power. At the same time, it is interesting to note that increasing M_{R} tends to improve the CE performance for cascaded channel training scheme, as opposed to the impact observed in RIS-TX scheme (recall Fig. 5). This is because, when M_{R} is large, the effective cascaded channel will combine more reflected paths and therefore enlarges the effective channel's magnitude.

V. Conclusion

This paper proposes a novel RIS CE scheme, where the RIS equipped with one TX RF-chain broadcasts pilots to other transceivers. Besides, we develop a GD-based pilot design method to reduce the MSE of CE. Numerical results show that our proposed channel training scheme is remarkably superior to the cascaded channel method. Besides, our GD-based pilot design outperforms the DFT codebook, which is believed to be optimal in the literature.

Appendix

A. Derivation of $\nabla_{\boldsymbol{\Theta}}\mathsf{g}(\boldsymbol{\Theta})$

Define $\tilde{\mathsf{g}}(\boldsymbol{\Phi})$ as the objective of $(\mathcal{P}2)$ and we firstly calculate $\frac{\partial}{\partial \boldsymbol{\Phi}}\tilde{\mathsf{g}}(\boldsymbol{\Phi})$. It can be seen that the Hadamard product and the Kronecker product make it difficult to derive. Notice that $\mathsf{Tr}\{\mathbf{A}\odot\mathbf{B}\}$ can be written as

$$\mathsf{Tr}\{\mathbf{A}\odot\mathbf{B}\}=\mathsf{Tr}\{\mathsf{Ddiag}(\mathbf{A})\mathbf{B}\}=\mathsf{Tr}\{\mathbf{A}\mathsf{Ddiag}(\mathbf{B})\}. \quad (25)$$

Via exploiting (25), the Hadamard product in (12) disappears.

To overcome the difficulty led by the Kronecker product, we first define and study the following derivatives

$$\mathbf{F}_{\mathrm{o}}(\mathbf{A},\mathbf{B},\mathbf{C},\mathbf{X}) \triangleq \frac{\partial}{\partial \mathbf{X}}\mathsf{Tr}\{\mathbf{C}((\mathbf{AXB})\otimes \mathbb{1}_N)\}, \tag{26}$$

$$\mathbf{F}_{\mathrm{e}}(\mathbf{A},\mathbf{B},\mathbf{C},\mathbf{X}) \triangleq \frac{\partial}{\partial \mathbf{X}}\mathsf{Tr}\{\mathbf{C}((\mathbf{AXB})\otimes \mathbf{I}_N)\}, \tag{27}$$

where the matrices $\mathbf{A}$, $\mathbf{B}$ and $\mathbf{X}$ are M-dimensional complex square matrices and $\mathbf{C}\in\mathbb{C}^{MN\times MN}$.

We firstly take (26) into consideration. Denote an M-dimensional matrix $\tilde{\mathbf{C}}$ whose (i,j)th element is given by $\sum_{s=(i-1)N+1}^{iN}\sum_{t=(j-1)N+1}^{jN}[\mathbf{C}]_{st}$. Then, $\mathsf{Tr}\{\mathbf{C}((\mathbf{AXB})\otimes \mathbb{1}_N)\}$ in (26) can be calculated as

$$\mathsf{Tr}\{\mathbf{C}((\mathbf{AXB})\otimes \mathbb{1}_N)\} = \sum_{m=1}^{M}[\tilde{\mathbf{C}}]_{m,:}\mathbf{AX}[\mathbf{B}]_{:,m}. \tag{28}$$

Hence, the derivative shown in (26) reads as

$$\begin{aligned}\frac{\partial}{\partial \mathbf{X}}\mathsf{Tr}\{\mathbf{C}((\mathbf{AXB})\otimes \mathbb{1}_N)\} &= \frac{\partial}{\partial \mathbf{X}}\sum_{m=1}^{M}[\tilde{\mathbf{C}}]_{m,:}\mathbf{AX}[\mathbf{B}]_{:,m}\\ =\frac{\partial}{\partial \mathbf{X}}\mathsf{Tr}\Big\{\sum_{m=1}^{M}[\mathbf{B}]_{:,m}[\tilde{\mathbf{C}}]_{m,:}\mathbf{AX}\Big\} &= (\mathbf{B}\tilde{\mathbf{C}}\mathbf{A})^{\mathrm{T}}.\end{aligned} \tag{29}$$

Following the similar procedure, function (27) has the same form as (26), where the (i,j)th element of $\tilde{\mathbf{C}}$ is $\mathsf{Tr}\{[\mathbf{C}]_{(i-1)N+1:iN,(j-1)N+1:jN}\}$ instead.

Via leveraging (26) and (27), the derivative $\frac{\partial}{\partial \mathbf{\Phi}}\tilde{\mathsf{g}}(\mathbf{\Phi})$ can be expressed as

$$\frac{\partial}{\partial \mathbf{\Phi}}\tilde{\mathsf{g}}(\mathbf{\Phi}) = \sum_{i=1}^{2}\mathbf{D}^{\mathrm{o}}_{\mathbf{\Phi},i} + \mathbf{D}^{\mathrm{e}}_{\mathbf{\Phi}}, \tag{30}$$

where

$$\begin{aligned}
&\mathbf{D}^{\mathrm{o}}_{\mathbf{\Phi},1}\triangleq\sum\nolimits_{k=1}^{K}\mathbf{F}_{\mathrm{o}}(\mathbf{W}^{\mathrm{H}}_{\mathrm{h},k}\mathbf{P},\mathbf{R}_{\mathrm{h},k}(\mathbf{\Phi P})^{*}\mathbf{W}_{\mathrm{h},k},\mathsf{Ddiag}(\mathbf{C}^{\mathrm{o}}_{1}),\mathbf{\Phi}),\\
&\mathbf{D}^{\mathrm{o}}_{\mathbf{\Phi},2} \triangleq -\sum\nolimits_{k=1}^{K}\mathbf{F}_{\mathrm{o}}(\mathbf{W}^{\mathrm{H}}_{\mathrm{h},k}\mathbf{P},\mathbf{R}_{\mathrm{h},k},\mathsf{Ddiag}(\mathbf{C}^{\mathrm{o}}_{2}),\mathbf{\Phi}),\\
&\mathbf{D}^{\mathrm{e}}_{\mathbf{\Phi}} \triangleq \mathbf{F}_{\mathrm{e}}(\mathbf{P},\mathbf{I}_{M_{\mathrm{R}}},\mathbf{C}^{\mathrm{e}}_{1}+\mathbf{C}^{\mathrm{e}}_{2}-\mathbf{C}^{\mathrm{e}}_{3},\mathbf{\Phi}),\\
&\mathbf{C}^{\mathrm{o}}_{1} \triangleq \mathbf{W}^{\mathrm{H}}_{\mathrm{G}}\mathbf{C}^{\mathrm{o}}_{1,1}\mathbf{W}_{\mathrm{G}},\\
&\mathbf{C}^{\mathrm{o}}_{1,1} \triangleq ((\mathbf{\Phi P})^{\mathrm{T}}\otimes\mathbf{I}_{M_{\mathrm{B}}})\mathbf{R}_{\mathrm{G}}((\mathbf{\Phi P})^{*}\otimes\mathbf{I}_{M_{\mathrm{B}}})+\mathbf{\Sigma}_{\mathrm{B}}\otimes\mathbf{I}_{M_{\mathrm{R}}},\\
&\mathbf{C}^{\mathrm{o}}_{2} \triangleq \mathbf{W}^{\mathrm{H}}_{\mathrm{G}}((\mathbf{\Phi P})^{\mathrm{T}}\otimes\mathbf{I}_{M_{\mathrm{B}}})\mathbf{R}_{\mathrm{G}},\\
&\mathbf{C}^{\mathrm{e}}_{1} \triangleq \mathbf{R}_{\mathrm{G}}((\mathbf{\Phi P})^{*}\otimes\mathbf{I}_{M_{\mathrm{B}}})\mathbf{W}_{\mathrm{G}}\mathbf{C}^{\mathrm{e}}_{1,1}\mathbf{W}^{\mathrm{H}}_{\mathrm{G}},\\
&\mathbf{C}^{\mathrm{e}}_{2} \triangleq \mathbf{R}_{\mathrm{G}}((\mathbf{\Phi P})^{*}\otimes\mathbf{I}_{M_{\mathrm{B}}})\mathbf{W}_{\mathrm{G}}\mathbf{C}^{\mathrm{e}}_{2,1}\mathbf{W}^{\mathrm{H}}_{\mathrm{G}},\\
&\mathbf{C}^{\mathrm{e}}_{3} \triangleq \mathbf{R}_{\mathrm{G}}\mathbf{C}^{\mathrm{e}}_{3,1}\mathbf{W}^{\mathrm{H}}_{\mathrm{G}},\\
&\mathbf{C}^{\mathrm{e}}_{1,1}\triangleq\sum\nolimits_{k=1}^{K}\mathsf{Ddiag}((\mathbf{W}^{\mathrm{H}}_{\mathrm{h},k}(\mathbf{\Phi P})^{\mathrm{T}}\mathbf{R}_{\mathrm{h},k}(\mathbf{\Phi P})^{*}\mathbf{W}_{\mathrm{h},k})\otimes\mathbb{1}_{M_{\mathrm{B}}}),\\
&\mathbf{C}^{\mathrm{e}}_{2,1} \triangleq \sum\nolimits_{k=1}^{K}\mathsf{Ddiag}((\mathbf{W}^{\mathrm{H}}_{\mathrm{h},k}\mathbf{\Sigma}_{\mathrm{U},k}\mathbf{W}_{\mathrm{h},k})\otimes\mathbb{1}_{M_{\mathrm{B}}}),\\
&\mathbf{C}^{\mathrm{e}}_{3,1} \triangleq \sum\nolimits_{k=1}^{K}\mathsf{Ddiag}((\mathbf{W}^{\mathrm{H}}_{\mathrm{h},k}(\mathbf{\Phi P})^{\mathrm{T}}\mathbf{R}_{\mathrm{h},k})\otimes\mathbb{1}_{M_{\mathrm{B}}}).
\end{aligned} \tag{31}$$

Moreover, recalling $\mathbf{\Phi}=e^{j\mathbf{\Theta}}$ and utilizing the chain rule, we have

$$\frac{\partial}{\partial \mathbf{\Theta}}\mathsf{g}(\mathbf{\Theta}) = j\frac{\partial}{\partial \mathbf{\Phi}}\tilde{\mathsf{g}}(\mathbf{\Phi})\odot e^{j\mathbf{\Theta}}. \tag{32}$$

Due to $\mathsf{g}(\mathbf{\Theta})$ real-valued, $\nabla_{\mathbf{\Theta}}\mathsf{g}(\mathbf{\Theta})$ can be calculated as

$$\begin{aligned}\nabla_{\mathbf{\Theta}}\mathsf{g}(\mathbf{\Theta}) &= \frac{\partial}{\partial \mathbf{\Theta}}\mathsf{g}(\mathbf{\Theta}) + \frac{\partial}{\partial \mathbf{\Theta}^{*}}\mathsf{g}(\mathbf{\Theta})\\ &= \frac{\partial}{\partial \mathbf{\Theta}}\mathsf{g}(\mathbf{\Theta}) + \left(\frac{\partial}{\partial \mathbf{\Theta}}\mathsf{g}(\mathbf{\Theta})\right)^{*} = 2\mathsf{Re}\Big\{\frac{\partial}{\partial \mathbf{\Theta}}\mathsf{g}(\mathbf{\Theta})\Big\}.\end{aligned} \tag{33}$$

B. Derivation of $\nabla_{\mathbf{p}}\mathsf{h}(\mathbf{p})$

Denote $\tilde{\mathsf{h}}(\mathbf{P})$ (recall that $\mathbf{P}=\mathsf{Diag}(\mathbf{p})$) as the objective of $(\mathcal{P}4)$ and we firstly investigate $\nabla_{\mathbf{P}}\tilde{\mathsf{h}}(\mathbf{P})$. Similar to the procedure shown in Appendix A, $\nabla_{\mathbf{P}}\tilde{\mathsf{h}}(\mathbf{P})$ can be given by

$$\nabla_{\mathbf{P}}\tilde{\mathsf{h}}(\mathbf{P}) = 2\mathsf{Re}\Big\{\sum_{i=1}^{2}\mathbf{D}^{\mathrm{o}}_{\mathbf{P},i}+\mathbf{D}^{\mathrm{e}}_{\mathbf{P}}\Big\}, \tag{34}$$

where

$$\begin{aligned}
&\mathbf{D}^{\mathrm{o}}_{\mathbf{P},1}\triangleq\sum\nolimits_{k=1}^{K}\mathbf{F}_{\mathrm{o}}(\mathbf{W}^{\mathrm{H}}_{\mathrm{h},k},\mathbf{\Phi}^{\mathrm{T}}\mathbf{R}_{\mathrm{h},k}(\mathbf{\Phi P})^{*}\mathbf{W}_{\mathrm{h},k},\mathsf{Ddiag}(\mathbf{C}^{\mathrm{o}}_{1}),\mathbf{P}),\\
&\mathbf{D}^{\mathrm{o}}_{\mathbf{P},2} \triangleq -\sum\nolimits_{k=1}^{K}\mathbf{F}_{\mathrm{o}}(\mathbf{W}^{\mathrm{H}}_{\mathrm{h},k},\mathbf{\Phi}^{\mathrm{T}}\mathbf{R}_{\mathrm{h},k},\mathsf{Ddiag}(\mathbf{C}^{\mathrm{o}}_{2}),\mathbf{P}),\\
&\mathbf{D}^{\mathrm{e}}_{\mathbf{P}} \triangleq \mathbf{F}_{\mathrm{e}}(\mathbf{I}_{M_{\mathrm{R}}},\mathbf{\Phi}^{\mathrm{T}},\mathbf{C}^{\mathrm{e}}_{1}+\mathbf{C}^{\mathrm{e}}_{2}-\mathbf{C}^{\mathrm{e}}_{3},\mathbf{P}),
\end{aligned} \tag{35}$$

and the notations in (35) have been defined in (31).

By exploiting $\mathbf{p}=\mathsf{diag}(\mathbf{P})$, we obtain

$$\nabla_{\mathbf{p}}\mathsf{h}(\mathbf{p}) = \mathsf{diag}(\nabla_{\mathbf{P}}\tilde{\mathsf{h}}(\mathbf{P})). \tag{36}$$

REFERENCES

[1] C. Pan and *et al.*, "An overview of signal processing techniques for RIS/IRS-aided wireless systems," *IEEE J. Sel. Topics Signal Process.*, vol. 16, no. 5, pp. 883–919, Aug. 2022.

[2] Q. Wu, S. Zhang, B. Zheng, C. You, and R. Zhang, "Intelligent reflecting surface-aided wireless communications: A tutorial," *IEEE Trans. Commun.*, vol. 69, no. 5, pp. 3313–3351, May 2021.

[3] Q. Wu and R. Zhang, "Intelligent reflecting surface enhanced wireless network via joint active and passive beamforming," *IEEE Trans. Wireless Commun.*, vol. 18, no. 11, pp. 5394–5409, Nov. 2019.

[4] Z. Zhou, N. Ge, Z. Wang, and L. Hanzo, "Joint transmit precoding and reconfigurable intelligent surface phase adjustment: A decomposition-aided channel estimation approach," *IEEE Trans. Commun.*, vol. 69, no. 2, pp. 1228–1243, Feb. 2021.

[5] N. K. Kundu and M. R. McKay, "Channel estimation for reconfigurable intelligent surface aided MISO communications: From LMMSE to deep learning solutions," *IEEE Open J. Commun. Soc.*, vol. 2, pp. 471–487, Mar. 2021.

[6] Z. Wang, L. Liu, and S. Cui, "Channel estimation for intelligent reflecting surface assisted multiuser communications: Framework, algorithms, and analysis," *IEEE Trans. Wireless Commun.*, vol. 19, no. 10, pp. 6607–6620, Oct. 2020.

[7] A. Taha, M. Alrabeiah, and A. Alkhateeb, "Enabling large intelligent surfaces with compressive sensing and deep learning," *IEEE Access*, vol. 9, pp. 44304–44321, Mar. 2021.

[8] S. Liu, Z. Gao, J. Zhang, M. D. Renzo, and M.-S. Alouini, "Deep denoising neural network assisted compressive channel estimation for mmWave intelligent reflecting surfaces," *IEEE Trans. Veh. Technol.*, vol. 69, no. 8, pp. 9223–9228, Aug. 2020.

[9] X. Chen, J. Shi, Z. Yang, and L. Wu, "Low-complexity channel estimation for intelligent reflecting surface-enhanced massive MIMO," *IEEE Wireless Commun. Lett.*, vol. 10, no. 5, pp. 996–1000, May 2021.

[10] M. Najafi, V. Jamali, R. Schober, and H. V. Poor, "Physics-based modeling and scalable optimization of large intelligent reflecting surfaces," *IEEE Trans. Commun.*, vol. 69, no. 4, pp. 2673–2691, Apr. 2021.

[11] Z. Zhang, L. Dai, X. Chen, C. Liu, F. Yang, R. Schober, and H. V. Poor, "Active RIS vs. passive RIS: Which will prevail in 6G?" Mar. 2022. [Online]. Available: https://arxiv.org/abs/2103.15154v5

[12] *Further advancements for E-UTRA physical layer aspects (Release 9)*. 3GPP TS 36.814, Mar. 2010.